SUPPLEMENTAL MATERIAL FOR:

Infrared and Visible Absolute and Difference Spectra of Bacteriorhodopsin Photocycle Intermediates

RICHARD W. HENDLER,* CURTIS W. MEUSE, MARK S. BRAIMAN,* PAUL D. SMITH, and JOHN W. KAKAREKA

Laboratory of Cell Biology, National Heart, Lung, and Blood Institute, National Institutes of Health, Bethesda, Maryland 20892 (R.W.H.); Biochemical Sciences Division, National Institute of Standards and Technology, Gaithersburg, Maryland 20899 (R.W.H., C.W.M.); Syracuse University Chemistry Department, Syracuse, New York 13244‐4100 (M.S.B.); National Institute of Biomedical Imaging and Bioengineering, National Institutes of Health, Bethesda, Maryland 20892 (P.D.S.); and Division of Computational Biosciences, Center for Information Technology, National Institutes of Health, Bethesda, Maryland 20892 (J.W.K.)

Received 18 March 2011; accepted 9 June 2011.

* Authors to whom correspondence should be sent. E-mail: mbraiman@syr.edu (for interpretations of IR spectra); rwh@helix.nih.gov (for isolation of absolute spectra and divided energy conservation functions of the M_F and M_S pathways).

This research was supported by the Intramural Research Program of the NIH, National Heart, Lung, and Blood Institute. Certain commercial equipment, instruments, or materials are identified in this paper to foster understanding. Such identification does not imply recommendation or endorsement by the National Institutes of Health or the National Institutes of Standards and Technology, or that the materials and equipment are necessarily the best available for the purpose.

We have used new kinetic fitting procedures to obtain infrared (IR) absolute spectra for intermediates of the main bacteriorhodopsin (bR) photocycle(s). The linear-algebra-based procedures of Hendler et al. (J. Phys. Chem. B, 105, 3319-3228 (2001)) for obtaining clean absolute visible spectra of bR photocycle intermediates were adapted for use with IR data. This led to isolation, for the first time, of

corresponding clean absolute IR spectra, including the separation of the M intermediate into its M_F and M_S components from parallel photocycles. This in turn permitted the computation of clean IR difference spectra between pairs of successive intermediates, allowing for the most rigorous analysis to date of changes occurring at each step of the photocycle. The statistical accuracy of the spectral calculation methods allows us to identify, with great confidence, new spectral features. One of these is a very strong differential IR band at 1650 cm^{-1} for the L intermediate at room temperature that is not present in analogous L spectra measured at cryogenic temperatures. This band, in one of the noisiest spectral regions, has not been identified in any previous time-resolved IR papers, although retrospectively it is apparent as one of the strongest L absorbance changes in their raw data, considered collectively. Additionally, our results are most consistent with Arg82 as the primary proton-release group (PRG), rather than a protonated water cluster or H-bonded grouping of carboxylic residues. Notably, the Arg82 deprotonation occurs exclusively in the M_F pathway of the parallel cycles model of the photocycle.

Index Headings: **Kinetic analysis; Reversible homogeneous model; Parallel cycles; Arginine 82 deprotonation; Proton release group; PRG; Flash photolysis; Purple membrane; Infrared spectroscopy.**

In addition to ground-state difference spectra, this supplement contains other important information. All of the difference spectra in the main paper's figures are between sequential intermediates (i.e., transitional difference spectra, TDS), whereas difference spectra in the published literature have been presented relative to the unphotolyzed or ground state BR (ground-state difference spectra, GDS). This Supplement provides a basis for more direct comparison to the latter (Figs. 1S, 2S, 3S, 4S). Figures 5S, 6S, and 7S display additional supporting information for the main paper.

Figure 1S below shows the GDS for intermediates M, N, and O, as M-(BR*), N-(BR*), and O-(BR*) in panels A, B, and C, respectively. Note that the GDS for L-(BR*) is shown in Fig. 4A of the main paper. Our GDS spectra are all similar to at least some of

the previously published TR-FTIR spectra of these intermediates. In comparing our GDS with those previously published, some differences are to be expected since our spectra were obtained with isolated intermediates, while those in the literature contained some degree of contamination from other species. The numbered references below correspond to the reference list in the main paper.

For example, the L-(BR*) transition from Fig. 4A of the main paper shows a particularly close resemblance to the fitted ($\tau 3$= 40 μs) spectrum of Fig. 3A in Rödig et al. 1999.[4] It also shows great resemblance to Fig. 4 of Dioumaev and Braiman, *J. Phys. Chem. B 101,* 1655-1662 (1997), and in Fig. 3 of Xiao et al., 2004.[27] A notable difference is the larger size of the positive band at 1651 cm^{-1} and the negative bands at 1661/1674 cm^{-1} in Ref. 27 of the main paper, relative to either Fig. 4A of the main paper here or Fig. 4 of Dioumaev and Braiman, 1997. This is likely due to more complete elimination in Ref. 27 of an "absorbance flattening" artifact that can result from the use of bR sample films of nonuniform thickness. The more complete avoidance of this artifact in Ref. 27 was made possible by the use of somewhat thinner samples overall, that have overall lower background absorbance near 1665 cm^{-1}.

The M-(BR*) spectrum in panel A of Fig. 1S, derived from the "combined" M_F and M_S spectra, shows particularly close resemblance to the fitted ($\tau 5$ = 544 μs) spectrum of Fig. 3A in Rödig et al. 1999.[4] It also closely resembles the single-time-slice 280-μs spectrum of wild-type bR in Fig. 3 of Rödig and Siebert, 1999;[35] as well as the M-bR fitted spectrum in Figs. 2 and 3 in Ref. 27. Once again, the 1661 cm^{-1} feature in the M-BR spectra in Ref. 27 is larger than in the other examples; and once again, this is most likely due to a reduction of the absorbance flattening artifact by use of thinner samples in Ref. 27.

The N-(BR*) spectrum in panel B of Fig. 1S is the most different, among our GDS, from any previously published TR-FTIR spectrum based on pH 7 data. It has been especially difficult for past workers to calculate an accurate N-(BR*) difference spectrum from data near pH 7, because the concentration of this intermediate never rises very high at neutral pH values (see Fig. 5 of the main paper). Nevertheless, the N-(BR*) difference spectrum in panel B below resembles, in its overall appearance, the N-BR difference spectrum in Fig. 2 of Ref. 29, which was obtained at pH 8.4. There are some intriguing differences in

the details, such as significantly shifted positions for some of the strongest vibrations (1558 and 1190 cm^{-1} in panel B below; 1553 and 1185 cm^{-1} in Ref. 29). These shifts could reflect an authentic structural difference between the N intermediates formed at pH 7 and 8.4. Alternatively they could represent a somewhat different mix of photointermediates that are present under the different conditions of the experiments. As discussed in the main text, we assert that the result in panel B in Fig. 1S below is the best representation of the GDS of an isolated N photoproduct state. The absence of the peak at 1763 cm^{-1} for Asp85, shows that N was free of contamination by M. No previously published GDS of N, calculated from IR data obtained at neutral pH, has been this free of M contamination.

The O-(BR*) spectrum in panel C of Fig. 1S resembles, in most of its prominent bands, the fitted ($\tau 8$ = 9.6 ms) spectrum of Fig. 3A in Rödig et al. 1999,[4] and to the pH 4 spectrum obtained in Fig. 2 of Ref. 29. As with the N-(BR) spectrum, the differences with respect to the published literature are authentic results of different pH values for the measurements, and/or a different (and, we assert, more complete) separation of the kinetically overlapping late photoproducts whose time courses are shown in Fig. 5 of the main paper.

As explained in the main paper, we use the term (BR*) to denote the spectral features of the last state that we can temporally resolve, under our measurement conditions, prior to formation of L. With our time resolution, this consists essentially of the unphotolyzed state.

In the main paper, BR (without the asterisk) indicates the structure of the asymptotically approached final product, many milliseconds after photolysis. That is, we have not temporally resolved the excited state of bR, which is what BR* traditionally designates. In Fig. 3 of the main paper, we show that the spectra we have obtained for (BR*) and BR are essentially the same.

An important aspect of comparing TDS to GDS is that the appearance and wavenumber values for peaks and troughs in the two types of spectra are likely to be significantly different. A prime example of this is seen in the most prominent features for O in the GDS at 1556 cm^{-1} and 1524.5 cm^{-1} of panel C in Fig. 1S in contrast to O in the TDS in panel D in Fig. 4 of the main paper. This is a simple consequence of using

different reference states for the subtraction. Intermediate O is more different from (BR*) at these two frequencies than it is from N. The marked differences in O and (BR*) are readily apparent in the absolute spectra shown in Fig. 2S.

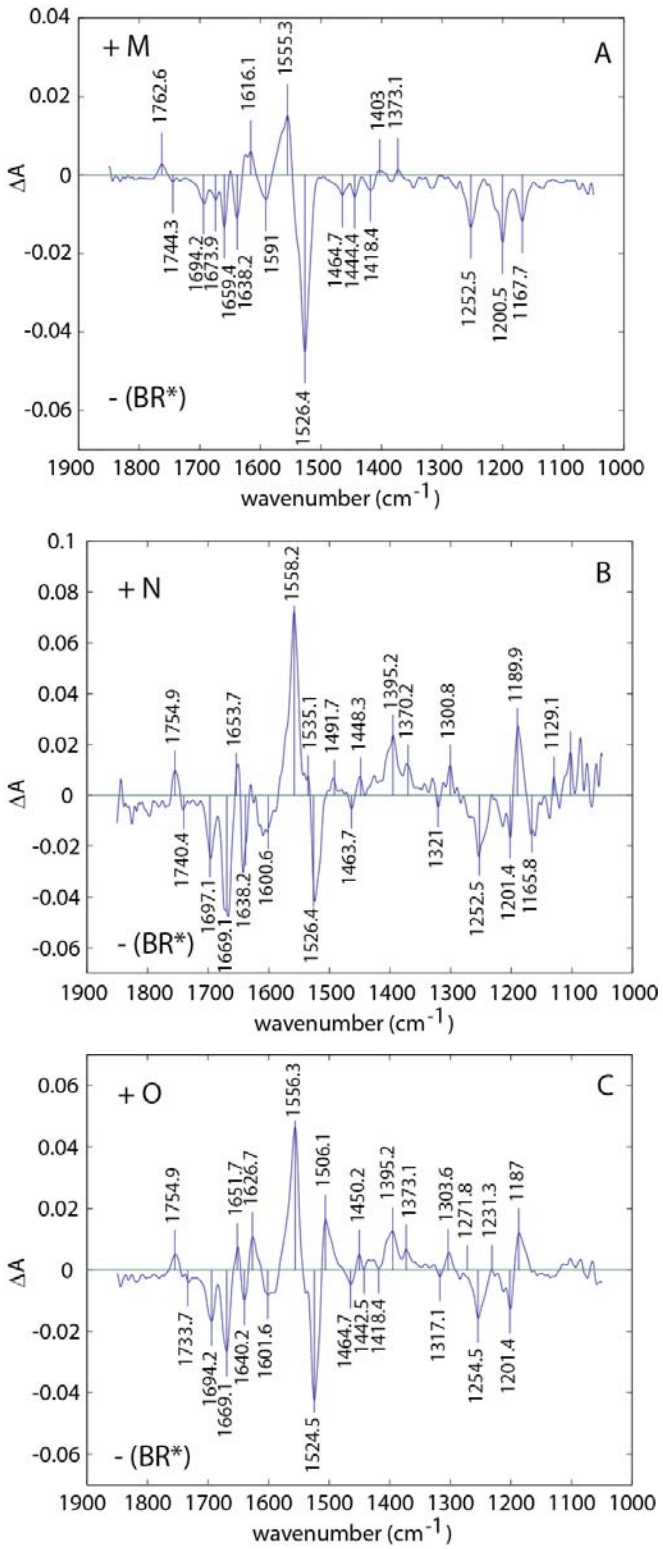

Fig. 1S. GDS for intermediates M, N, and O. Panel A should be compared with Fig. 4B in the main paper. Panel B should be compared with Figs. 4C and 10C in the main paper. Panel C should be compared with Figs. 4D and 10D in the main paper.

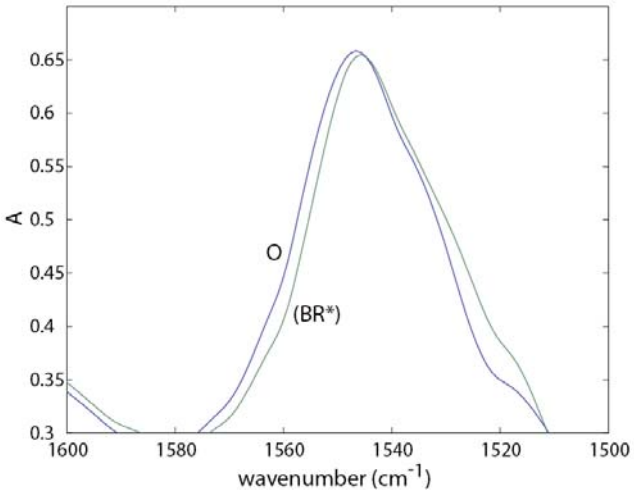

Fig. 2S. Absolute spectra for O (blue) and (BR*) in Amide II region.

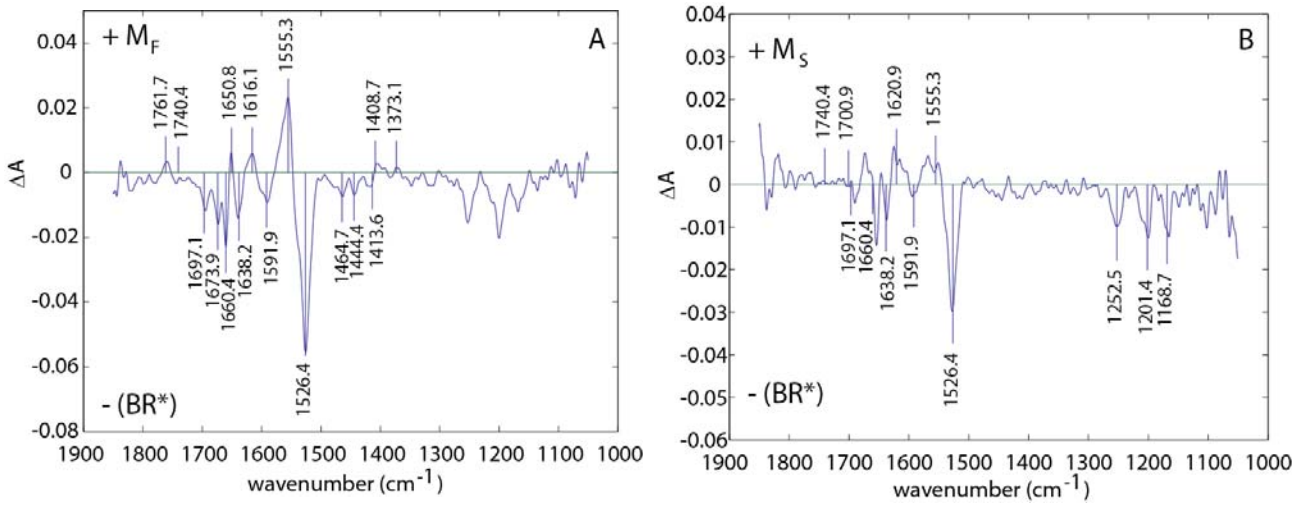

Fig. 3S. GDS for intermediates M_F (panel A) and M_S (panel B).

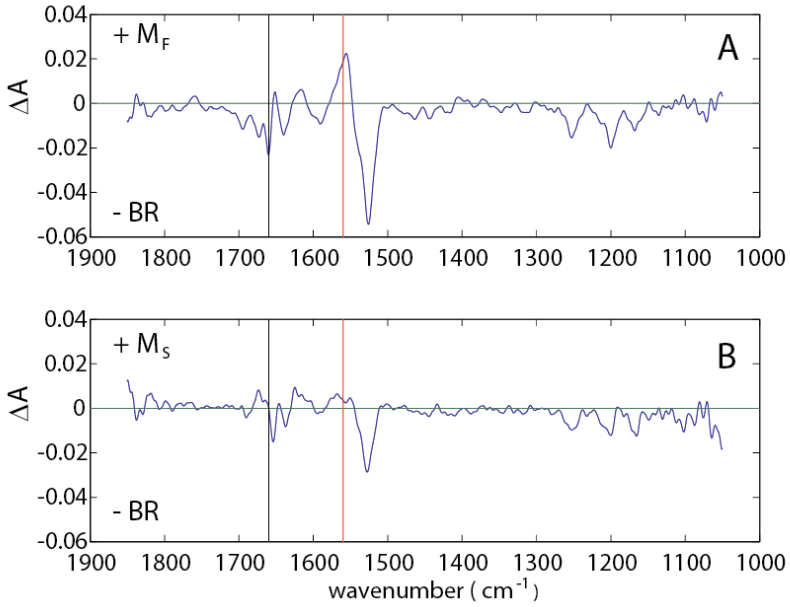

Fig. 4S. M_F – (BR*) and M_S – (BR*) spectra, are redrawn to emphasize the positions at 1660 cm^{-1} (black vertical line) and at 1560 cm^{-1} (red vertical line).

Comparison of kinetics measured by IR and visible spectroscopies

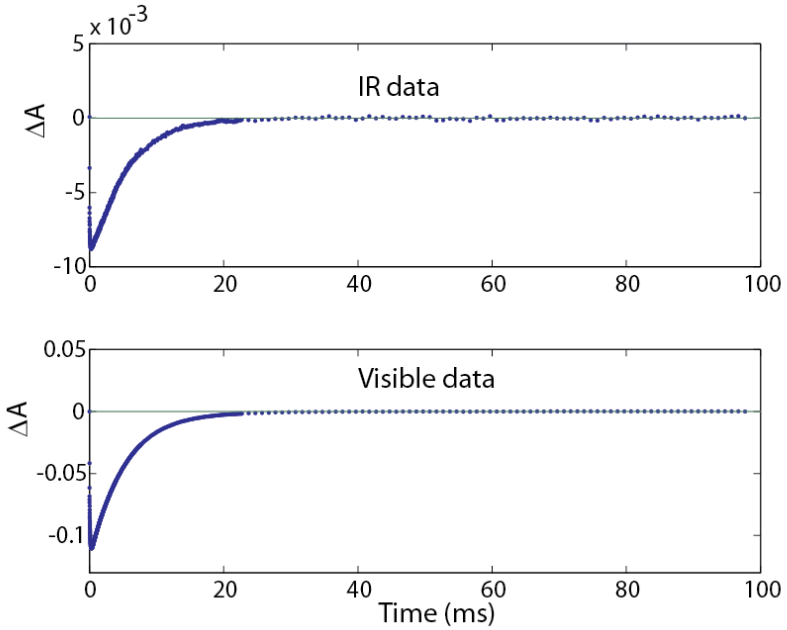

Fig. 5S. Time courses for BR changes in the photocycle measured at 1526 cm^{-1} in the IR and at 568 nm in the visible range. The IR data were obtained from an average of 800 repeats. The visible data were averaged from 200 repeats.

Figures 6S and 7S show other IR marker bands generally identified with BR and M follow the same kinetics as the known visible marker bands.

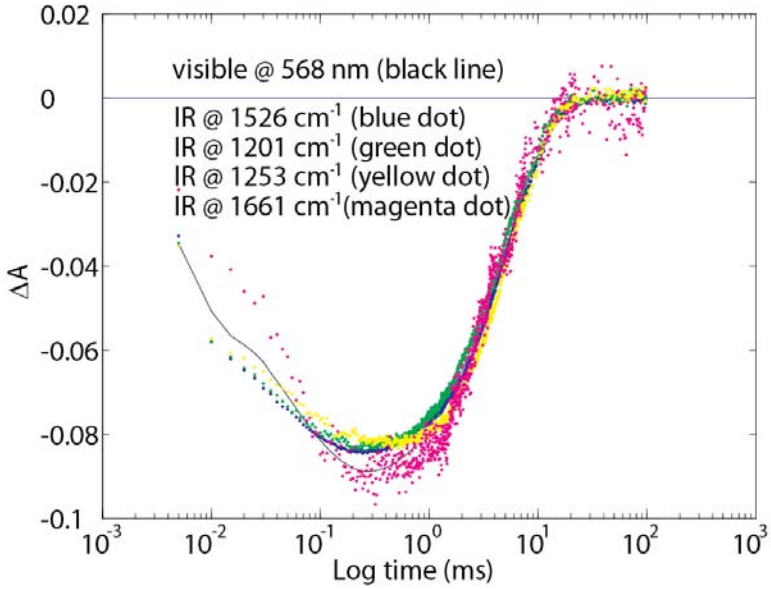

Fig. 6S. IR markers for BR. Scaled time courses for specific troughs prominent in the L-(BR*) difference spectrum in Fig. 4A of the main paper compared to the visible time course at 568 nm which is characteristic for BR (black line). The feature at 1526 cm^{-1}, for example, represents the C=C stretching vibration of the all-trans retinylidene chromophore of BR.

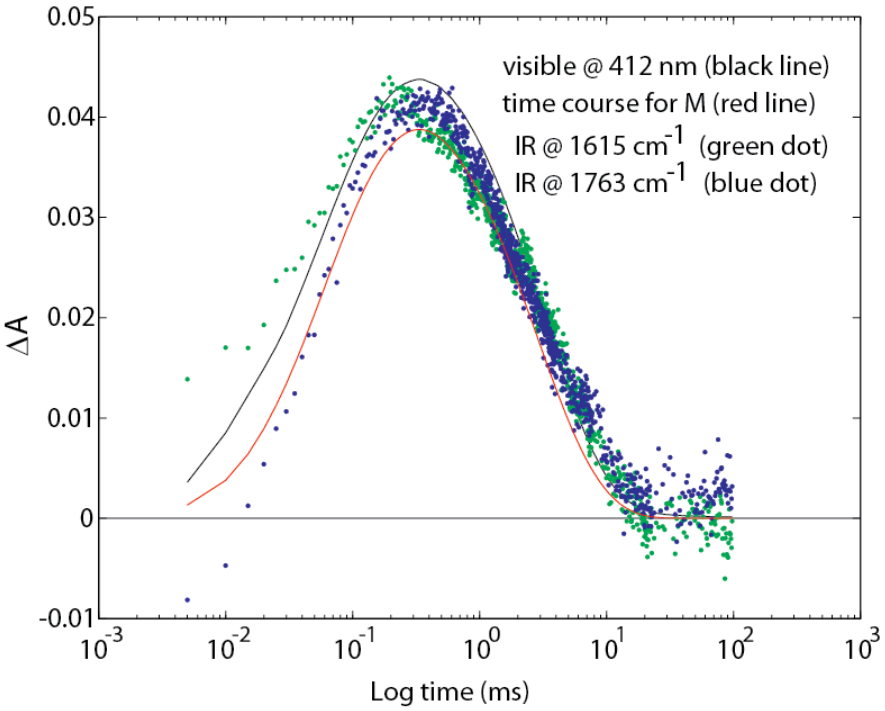

Fig. 7S. IR markers for M. Scaled time courses for example frequencies in M minus L difference spectra in Fig. 5B, compared to the visible time course at 412 nm which is characteristic for M (black line) and to the model-specific fitted time course for M (red line). The feature at 1763 cm^{-1}, for example, is from protonated Asp85.